Spectroscopy of Hydrothermal Reactions. 12. Acid-Assisted Hydrothermolysis of Aliphatic Nitriles at 150−260 °C and 275 bar

A. J. Belsky and T. B. Brill*

Department of Chemistry and Biochemistry, University of Delaware, Newark, Delaware 19716

Received: November 9, 1998; In Final Form: February 12, 1999

The conversion of four alkyl nitrile compounds, RCN, to the corresponding carboxylic acids and ammonia in fluid H_2O at 150−260 °C under 275 bar is described. The reaction rate was increased by the addition of 0.3−1.0 N HCl. The kinetics and pathways of the reactions were determined in real time by IR spectroscopy with a sapphire−titanium flow cell. Ex situ IR and Raman spectral data following batch reaction aided in establishing the reaction pathways. When R = CH_3−, CH_3CH_2−, and $(CH_3)_2CH$−, the relatively simple conversion to RCO_2H and NH_3 occurred and was modeled by two protonation equilibria and two forward reactions. When R═$HOC(O)CH_2$−, a more complex pH-dependent reaction took place because of the presence of two functional groups. The carboxylate group reacted at high pH, whereas the nitrile group reacted at low pH. The kinetics of these reactions were determined in real time, and the Arrhenius parameters were obtained. The activation energy for the hydrothermolysis of the nitriles qualitatively correlates with ν(CN), indicating that the electron-donating power of R is a factor in the rate of reaction. Consistent with this observation is the fact that a Taft plot is linear when the electronic effect of R is weighed more heavily than the steric contribution. This was not the case when R═$HOC(O)CH_2$−, where a different transition state is proposed.

Introduction

The reactions of the nitrile functional group in aqueous solution have potentially important ramifications in nature. One popular hypothesis is that Strecker synthesis, or a closely related reaction, provided easy access to α-amino- and α-hydroxycarboxylic acids and were essential to the early life-forming process.[1−4] Aldehydes and/or ketones react with NH_3 and HCN in this reaction to form α-amino- and α-hydroxynitriles, which, in turn, react with H_2O to liberate the corresponding substituted carboxylic acids. In this manner the hydrolysis of aliphatic nitrile groups potentially has a role in the origins of life, although questions have been raised about the role of Strecker synthesis in a major source of these essential carboxylic acids, which is in the submarine hydrothermal vent.[5] Typical intrinsic conditions in these vents are T = 200−300 °C and P = 200−300 bar.[6,7] Thermodynamic considerations suggest that the aldehyde and ketone reactants may have insufficient concentrations in this hostile environment for amino and hydroxy acids to form abundantly by this pathway. Carboxylic acids containing the nitrile group are also known to form in natural waters after chlorination of humic acid.[8]

Nitrile-containing compounds are extensively used in the manufacture of industrial and commercial products. As such, the hydrothermolysis of organonitrile compounds is important if waste streams containing these compounds are to be remediated by hydrothermal methods, including wet-air oxidation and supercritical water oxidation.

A flourish of studies appeared in the mid-century on the acid-accelerated kinetics and mechanism of hydrolysis of organonitriles, RCN.[9−16] These studies showed that nitriles only slowly hydrolyze to form amides in the neutral solution. For example, the half-life of acetonitrile in H_2O at 65 °C is about 300 days.[7] On the other hand, a high concentration of acid (e.g., >2 N HCl) can be used to accelerate this conversion. The consecutive pseudo-second-order reactions 1 and 2[15] occur in acid solution in which the protonated nitrile RC═NH^+ and protonated amide are believed to be the reactive species.

$$\mathrm{RCN} + \mathrm{H_2O} \xrightarrow[\mathrm{H^+}]{k_1} \mathrm{RC(O)NH_2} \quad (1)$$

$$\mathrm{RC(O)NH_2} + \mathrm{H_2O} \xrightarrow[\mathrm{H^+}]{k_2} \mathrm{RCO_2H} + \mathrm{NH_3} \quad (2)$$

The value of k_2 is about 15 times larger than k_1 in 4 N HCl.[9,17] Protonation of the nitrile apparently enhances the susceptibility of the electrophilic carbon atom to nucleophilic attack by H_2O and thereby shortens the reaction time at 50−100 °C to a few hours.

Interest in nitrile hydrolysis was rekindled recently by the potential use of hydrothermal methods to remediate waste streams[18−20] and to convert biomass material[21] containing organonitriles. These studies have been conducted by heating of the nitrile in water in a batch-mode tube reactor, cooling after a prescribed reaction time, and determining the products off-line by various analytical techniques, such as GC and GC/MS. An attempt has been made in the work described herein to advance the understanding of the kinetics and mechanisms of acid-assisted hydrothermolysis of aliphatic nitrile compounds by using real-time IR spectroscopy in a flow cell at reaction conditions. Temperatures of 150−260 °C at a pressure of 275 bar were used. The results for acid-assisted hydrothermolysis of several simple aliphatic nitriles RCN (R═CH_3−, CH_3CH_2−, and $(CH_3)_2CH$−) were used to validate this method for use in the study of the more complex hydrothermolysis scheme of cyanoacetic acid, $NCCH_2CO_2H$. In contrast to previous flow reactor spectroscopic studies,[22−31] this is the first study in which

* Author for correspondence. E-mail: brill@udel.edu.

10.1021/jp984364d CCC: $18.00
Published on Web 03/31/1999

an acid catalyst has been deliberately added to the reaction at hydrothermal conditions.

Experimental Section

Cyanoacetic acid ($HOC(O)CH_2CN$), acetonitrile (CH_3CN), propionitrile (CH_3CH_2CN), isobutyronitrile ($(CH_3)_2CHCN$), isobutyramide, isobutyric acid, acetamide, acetic acid, propylamide, and propionic acid were all obtained from Aldrich Chemical Co. Each had +98% purity and was used as received, except for acetonitrile, which was dried over molecular sieves. Malonamic acid ($H_2NC(O)CH_2CO_2H$) was prepared by the method of Galat.[32] Solutions were then made from Milli-Q H_2O that had been sparged with Ar to remove atmospheric gases. Concentrations were 1.0 *m* except for the less-soluble isobutyronitrile, which was studied at 0.5 *m*. Added HCl was 0.30 N as determined by multiple titrations with a KHP-standardized NaOH solution.

The laboratory-scale flow reactor spectroscopy cell[22,23] was constructed of grade 2 titanium into which two 0° sapphire windows were seated. Gold-foil washers were compressed at each interface to form the seals. The solution flowed in a flat duct that was created between the two sapphire windows by a slot cut into the gold washer that separated the windows. The path length of the cell (the thickness of the flat duct) was (30−35) ± 1 μm as determined by the absorbance of a known concentration of aqueous CO_2 flowing through the cell.[33] The temperature was controlled (±1 °C) by using PID controllers, the pressure was controlled (±1 bar) by a pneumatic bleed-and-lock system, and the constant flow rate maintained with an Isco syringe pump.[23] A single liquid phase was maintained at all times.

To investigate the kinetics of reactions, flow rates were used such that plug−flow conditions could be assumed to exist.[22,34] The flow rates used resulted in residence times of 3−60 s and degrees of conversion of about 50% or less. The true residence time was obtained by dividing the internal volume of the cell (entrance tube and flat duct), which was 0.0819 cm^3, by the expression [volume flow rate × $\rho_{25°C}/\rho_T$]. The density correction is needed because the density of H_2O, ρ_T, depends on the temperature (e.g., $\rho_{150°C} = 0.93$ g/cm^3, $\rho_{260°C} = 0.81$ g/cm^3 at a constant pressure of 275 bar).

A Nicolet 60SX FTIR spectrometer equipped with a liquid-N_2-cooled MCT-A detector was used for real-time IR spectral measurements in the flow reactor. Thirty-two spectra were summed at 4 cm^{-1} resolution (~10 s collection time) at each flow rate and temperature. The IR spectra were normalized with background spectra of pure H_2O recorded at the same conditions. The carbonyl stretching modes of the carboxylic acid and amide were partially visible but could not be quantified reliably because of the interference from the O−H bending mode of H_2O and the sapphire cutoff in the vicinity of 1700 cm^{-1}. The IR-active CN stretch of the nitriles (~2250 cm^{-1}) and the CO_2 product (2343 cm^{-1})[23] in the case of $NCCH_2CO_2H$ were resolved at each reaction condition using Peakfit software (Jandel Scientific) and a Matlab program. Four-parameter Voigt functions were employed to fit these bands. Three or more sets of data were recorded for each nitrile to establish the average concentration and the standard deviation. Kinetic models requiring a running tally of $[H^+]$ during the reaction were solved in small time increments with Euler's method in Lotus 1-2-3. A weighted least-squares regression was used to determine the value and error of each rate constant and the Arrhenius parameters, with care taken when converting the error into log space.[35,36]

Several batch reaction mode experiments were conducted with the reactant (1.0 or 0.5 *m*) and 0.3 N HCl in titanium tubes having an internal volume of 12 cm^3. These tube reactors were then heated in a fluidized sand bath for selected time periods of 5 min or more.[37] IR and/or Raman spectroscopy of the cooled solution was used to determine the products. These IR spectra were collected on a Nicolet 560ESP spectrometer equipped with a liquid-N_2-cooled MCT-A detector. Raman spectra were collected using a Kaiser Optical Systems dispersive spectrometer with a thermoelectrically cooled CCD detector. A 50 mW, diode-pumped, frequency-doubled, Nd:YAG laser was used for excitation at 532 nm. Five scans (10 s each) were recorded and averaged to give each spectrum.

TABLE 1: Taft Electronic and Steric Parameters for the Nitrile Substituents

R	σ^* [a]	E_s [b]
CH_3-	0	0
CH_3CH_2-	−0.1	−0.07
$(CH_3)_2CH-$	−0.19	−0.47
$HOC(O)CH_2-$	1.08	−0.75[c]

[a] Reference 39. [b] Reference 40. [c] Reference 31.

The Taft plots[38] required the use of Sigma Plot (Jandel Scientific) to solve for the steric (δ) and electronic (ρ) weighting parameters. The steric (E_s) and electronic (σ^*) constants for the R groups of the nitriles are listed in Table 1.[28,39,40]

Results and Discussion

Choice of the Catalyst. As noted in the Introduction, the addition of a strong acid has long been known to accelerate the decomposition of organonitrile compounds. Since H^+ is consumed by the eventual products (e.g., NH_3), it is potentially confusing to refer to the overall reaction as acid-catalyzed, even though H^+ is conserved in the initial step. With this in mind, the convention of referring to the reaction as "acid-catalyzed" will be retained here. The counterion and concentration of the acid catalyst are important factors in nitrile hydrolysis on the basis of past studies of the acid (H_2SO_4, HNO_3, HBr, and HCl) and concentration (0.3−22.2 N).[9−11,13] The identity of the counterion affects the overall reaction pathway, and large changes in the acid concentration affect the ratio of the consecutive rates k_1 and k_2 (eqs 1 and 2). For example, $k_2 \gg k_1$ at less than 4 N HCl, whereas the reverse is true at much larger acid concentrations.[10,11] Thus, exploratory work was conducted to choose the appropriate acid and concentration for this work. In turn, this choice dictated the cell type.

Of the four commonly used acid catalysts listed above, HNO_3 is known to oxidize and hydrolyze aliphatic nitriles to CO_2 and other products.[41] H_2SO_4 has been shown to be a less effective nitrile hydrolysis catalyst than HCl[9] and also to act as a nucleophile when its concentration is high.[42] Therefore, HCl was chosen as the catalyst. HCl corrodes stainless steel, however, necessitating the use of spectroscopy cells constructed of titanium and gold, which are relatively unreactive toward the chloride ion.[43] A relatively low HCl concentration (0.3 N) provides nearly equal rates throughout the nitrile and amide hydrolysis reactions, but the carboxylic acid and ammonia products buffer the system and NH_3 consumes the catalyst in the later stages.

Spectral Determination of the Reaction Pathways. Raman spectroscopy helps identify the products from batch reaction of the alkyl nitriles after 20 min in 0.3 N HCl (Figures 1−3). The formation of the corresponding carboxylic acid is revealed along with the presence of unreacted parent nitrile. The absence of Raman modes for the amide supports the earlier finding[10,11] that hydrolysis of the amide is faster than the nitrile (i.e., $k_2 \gg$

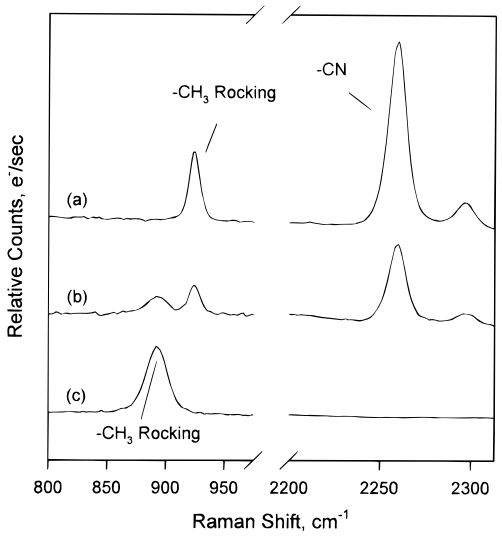

Figure 1. Raman spectra of (a) CH_3CN in 0.3 N HCl at 25 °C; (b) 1.0 *m* CH_3CN in 0.3 N HCl after heating in a tube reactor at 230 °C for 20 min; (c) acetic acid in 0.3 N HCl. The heated solution shows the presence of unreacted nitrile and acetic acid (reaction 3). The peak at 2295 cm^{-1} is an overtone/combination band of CH_3CN.

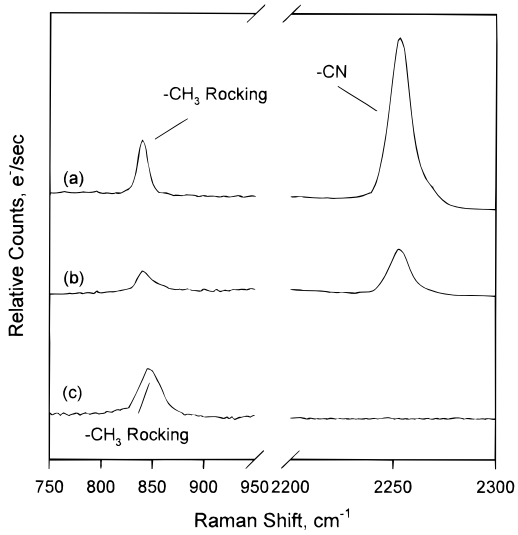

Figure 2. Raman spectra of (a) CH_3CH_2CN in 0.3 N HCl at 25 °C; (b) 1.0 *m* CH_3CH_2CN in 0.3 N HCl after heating in a tube reactor at 230 °C for 20 min; (c) propionic acid in 0.3 N HCl. Partial conversion by reaction 3 is indicated in (b).

k_1). The global reaction 3, which is the net reaction of reactions 1 and 2, describes the hydrolysis of simple alkyl nitriles (R= CH_3-, CH_3CH_2-, and $(CH_3)_2CH-$) because the amide formed has a low steady-state concentration.

$$RCN + 2H_2O \rightarrow RCO_2H + NH_3 \qquad (3)$$

In contrast to the simple alkyl nitriles, the hydrothermal reaction of cyanoacetic acid is potentially more complicated because both the cyano and carboxylate functional groups can react (reactions 3 and 4) depending on the experimental conditions used. Previous kinetic and mechanistic studies of cyanoacetic acid,[31] malonamic acid,[31] and malonic acid[28] in neutral H_2O at high temperature and pressure have confirmed the occurrence of reaction 4.

$$RCO_2H \rightarrow RH + CO_2 \qquad (4)$$

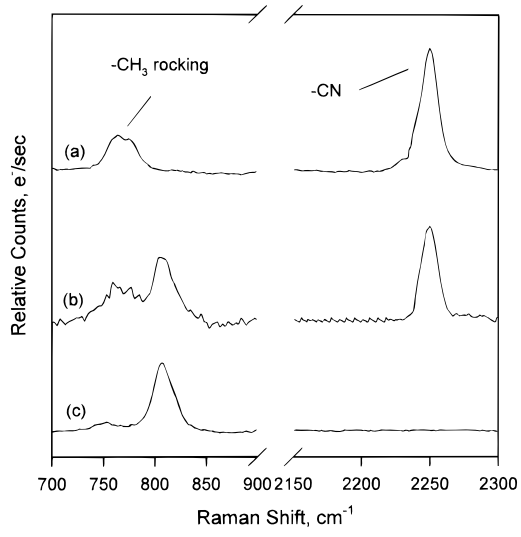

Figure 3. Raman spectra of (a) $(CH_3)_2CHCN$ in 0.3 N HCl at 25 °C; (b) 0.5 *m* $(CH_3)_2CHCN$ in 0.3 N HCl after heating in a tube reactor at 230 °C for 20 min; (c) isobutyric acid in 0.3 N HCl. Partial conversion of reaction 3 is indicated in (b).

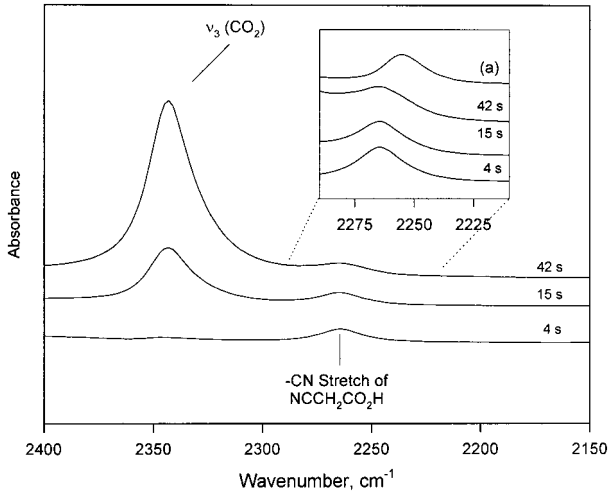

Figure 4. Time series of IR spectra for 1.0 *m* $NCCH_2CO_2H$ in 0.3 N HCl in the flow cell at 210 °C under 275 bar. The spectra show an increase in CO_2 (2343 cm^{-1}) with a decrease in the nitrile stretch (2265 cm^{-1}); (a) in the insert shows the position of the nitrile in CH_3CN if step A had occurred. Since the nitrile does not shift, step A cannot be occurring.

On the other hand, the addition of a strong acid favors the occurrence of reaction 3 at a lower temperature and has been used to produce malonic acid from cyanoacetic acid.[41] The more extensive reaction pathway shown in Scheme 1 thereby becomes possible depending on the reaction conditions.

The IR spectroscopic data from the flow cell at 150−260 °C help refine the conditions for Scheme 1. Step A has been proven by IR spectroscopy to occur in neutral H_2O solution.[31] On the other hand, Figure 4 shows that in 0.3 N HCl, the CN stretch of $NCCH_2CO_2H$ at 2265 cm^{-1} does not shift to 2256 cm^{-1}, which would have indicated the formation of CH_3CN,[31] but CO_2 forms. This seeming contradiction is explained by the fact that the CO_2 may also be formed by the combination of steps B and C in which no CH_3CN forms. Three results support steps B and C. First, the intensity of the CN stretch decreased with time without a shift in the frequency, which indicates that step B, rather than step A, took place in 0.3 N HCl solution (Figure 4). Second, the rate of formation of CO_2 is observed to be slower by a factor of 2 after 30 s than is predicted by the kinetics of

SCHEME 1

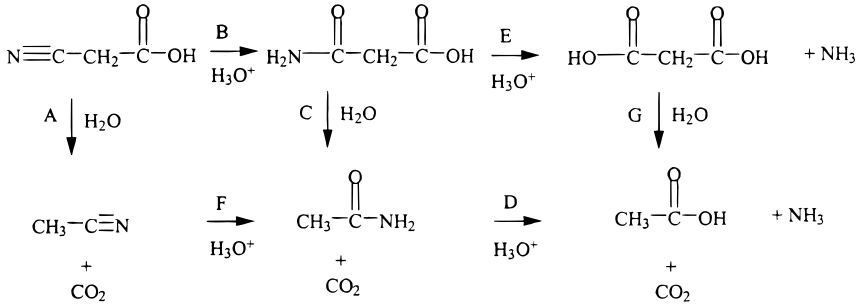

SCHEME 2

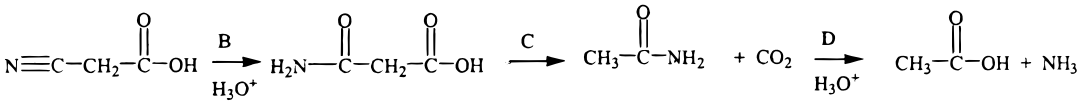

SCHEME 3

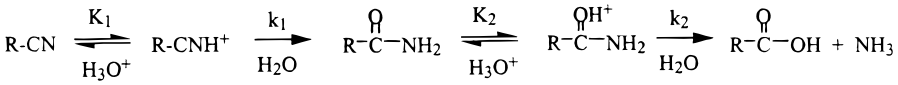

step A.[31] Third, the rate of decarboxylation of malonamic acid (step C) is faster at the conditions used in this work than the alternative hydrolysis pathway to malonic acid (step E).[31] Discussion of step E is deferred until the following paragraph in order to complete the discussion of steps A−C here. As noted above, step A occurs in neutral H_2O solution. Indeed, when the reaction had progressed sufficiently to consume the acid catalyst and the pH had increased toward neutral, the decarboxylation of cyanoacetic acid (step A) occurred. This switch from step A to steps B and C is demonstrated by progressively increasing the HCl concentration from 0.01 to 1.0 N as shown in Figure 5. The explanation at the low $[H^+]$ is that the catalyst was quickly consumed by NH_3 formed in Scheme 1, causing the pH to increase, which, in turn, favors step A. At a higher $[H^+]$, ample acid was present at all times so that steps B and C exclusively occur. This later observation is consistent with the results of Darensbourg et al.,[44] who used metal catalysts to decarboxylate $NCCH_2CO_2H$ and noted that the presence of a strong acid shuts down the decarboxylation process. In summary, the main point is that step A is stopped by the presence of strong acid in favor of steps B and C.

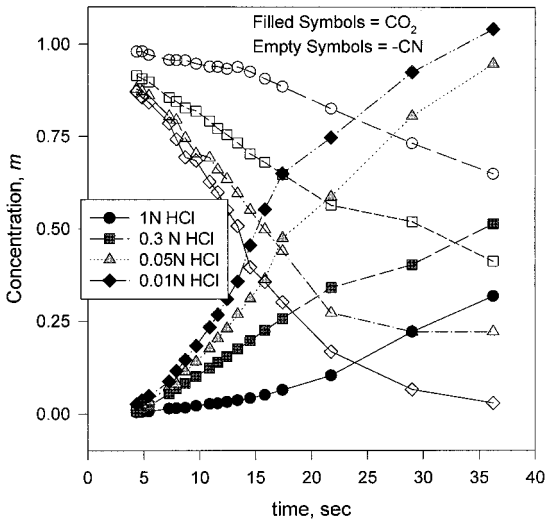

Figure 5. Plot of the concentration of the nitrile and CO_2 measured in the IR spectroscopy flow cell of $NCCH_2CO_2H$ at 230 °C and 275 bar showing that the reaction slows due to the shift from step A to step B as the $[H^+]$ concentration is increased.

The malonamic acid product of step B and has two possible decomposition pathways, decarboxylation to acetamide (step C) or hydrolysis to malonic acid (step E). Previous studies at <90 °C showed that malonamic acid only converts to malonic acid (step E) in concentrated HCl.[41] At lower HCl concentrations, however, Hall showed that the rate of decarboxylation of malonamic acid (step C) was essentially independent of the HCl concentration,[45] a finding that was also confirmed at hydrothermal conditions.[31] Therefore, the decarboxylation step C is the only pathway that occurs at the temperatures and HCl concentrations used in this work. Since the acetamide product of step C has only one pathway to hydrolyze to acetic acid (step D), the acid-catalyzed decomposition pathway of $NCCH_2CO_2H$ is complete. Scheme 2 is the simpified version of Scheme 1, which applies in 0.3 N HCl at hydrothermal conditions. Acetic acid is refractory at these conditions.[46,47] The other product, NH_3, is also refractory at these conditions except that it consumes the H^+ catalyst, which causes step A of Scheme 1 to become increasingly important as the pH approaches neutral.

Kinetic Determinations. Scheme 3 is the proposed acid-catalyzed hydrothermolysis mechanism of the simple alkyl nitriles, RCN (R=CH_3−, CH_3CH_2−, and $(CH_3)_2CH$−). It is generally agreed that protonation of the nitrile and amide facilitates nucleophilic attack by H_2O and that this is the function of the acid catalyst.[48] Equilibria K_1 and K_2 both favor the neutral (left-hand) form because the nitrile group is only weakly basic.[42,49] The rate expression for the disappearance of RCN (eq 5) is considered to be pseudo-second-order with respect to $[H^+]$ and [RCN].[13,18−20]

$$-\mathrm{d[RCN]}/\mathrm{d}t = k_1K_1[\mathrm{H_2O}][\mathrm{H^+}][\mathrm{RCN}] = k_1'[\mathrm{H^+}][\mathrm{RCN}] \quad (5)$$

$$-\mathrm{d[RC(O)NH_2]}/\mathrm{d}t = k_2K_2[\mathrm{H_2O}][\mathrm{H^+}][\mathrm{RC(O)NH_2}] = k_2'[\mathrm{H^+}][\mathrm{RC(O)NH_2}] \quad (6)$$

Likewise, the disappearance of the amide (eq 6) is pseudo-second-order, but these expressions disguise the subtle complexities of the reaction.

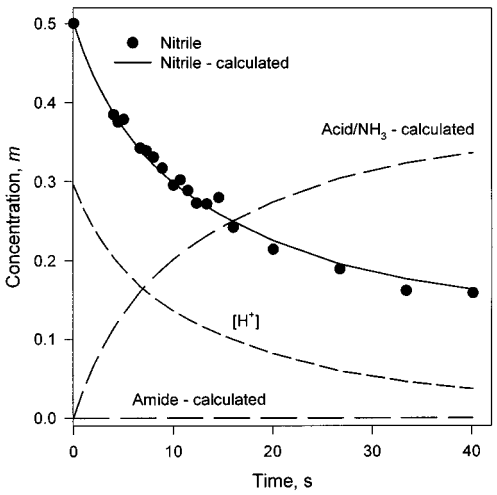

Figure 6. Calculated and actual concentrations for 0.5 *m* isobutyronitrile in 0.3 N HCl (eq 5) at 240 °C under 275 bar.

As the reaction progresses, the acid catalyst is gradually consumed by the association of the H^+ with NH_3 (reaction 7).

$$NH_3 + H_3O^+ \overset{K_b}{\rightleftharpoons} NH_4^+ + H_2O \quad (7)$$

$$RC(O)OH + H_2O \overset{K_a}{\rightleftharpoons} RC(O)O^- + H_3O^+ \quad (8)$$

$$HCl + H_2O \overset{K_c}{\rightleftharpoons} Cl^- + H_3O^+ \quad (9)$$

The acid−base equilibrium involving the carboxylic acid, ammonia, and $[H^+]$ buffers the solution from the initial pH of about 0.5 to about pH = 3 in the later stage. For comparison 0.5 *m* $NCCH_2CO_2H$ has a pH of 1.5 at 200 °C. As part of establishing the running pH value during the reaction, the equilibrium constants K_a, K_b, and K_c (eqs 7, 8, and 9) at the reaction temperature were determined from literature values at lower temperature[50,51] by the iso-Coulombic extrapolation method.[52] This method takes into account the effect of changing K_W of H_2O[53] on the ionization constants of the acids and bases. Figure 6 shows the apparent rate of disappearance of 0.5 *m* $(CH_3)_2CHCN$ at 230 °C in the IR flow reactor. The rate clearly decreases as the reaction proceeds as a result of the removal of $[H^+]$ by reaction 7. This change is the basis for determining the apparent nitrile hydrolysis rate, k_1', in eq 5. $[H^+]$ is known by paramatrizing eq 10 at all times and temperatures used.

$$[H^+] + \frac{B_T[H^+]}{K_b + [H^+]} = \frac{K_W}{[H^+]} + \frac{K_aB_T}{K_a + [H^+]} + \frac{K_cC_T}{K_c + [H^+]} \quad (10)$$

Equation 10 is determined from the conservation of charge (eq 11) during the reaction.

$$[H^+] + [NH_4^+] = [Cl^-] + [RCO_2^-] + [OH^-] \quad (11)$$

The total carboxylic acid concentration is A_T (=RCO_2H + RCO_2^-), the total concentration of ammonia is B_T(=NH_3 + NH_4^+), and the total of concentration HCl is C_T. Because the carboxylic acid and ammonia are produced simultaneously in reaction 2, $A_T = B_T$. Therefore, only B_T appears in eq 10. Equilibration reactions 7−9 occur much faster than the rate-determining step of Scheme 1, so acid−base equilibrium was assumed at all times.

TABLE 2: Pseudo-Second-Order Rate Constants for the Hydrothermolysis of RCN at 275 bar in the IR Flow Reactor

	k, kg/(mol s) × 100			
T, °C	R = CH_3− (1.0 *m*)	R = CH_3CH_2− (1.0 *m*)	R = $(CH_3)_2CH$− (0.5 *m*)	R = $HOC(O)CH_2$− (1.0 *m*)
150		0.22 ± 0.06		0.051 ± 0.008
160		0.39 ± 0.03		0.12 ± 0.02
170		0.72 ± 0.05	1.4 ± 0.3	0.27 ± 0.03
180		1.3 ± 0.1	1.8 ± 0.1	0.66 ± 0.08
190		1.8 ± 0.5	2.5 ± 0.10	1.5 ± 0.2
200	0.79 ± 0.19	3.5 ± 0.7	3.5 ± 0.5	3.4 ± 0.5
210	1.6 ± 0.4	4.7 ± 1.4	7.3 ± 4.2	7.5 ± 1.4
220	3.0 ± 1.0	10 ± 4	14 ± 3	16 ± 3
230	6.5 ± 1.7	14 ± 6	18 ± 4	38 ± 7
240	12 ± 3	20 ± 7	24 ± 5	
250	18 ± 2	29 ± 9	31 ± 6	
260	31 ± 4	43 ± 11	40 ± 8	

TABLE 3: ν(CN) and Arrhenius Parameters for Decomposition of RCN

R	E_a kcal/mol	ln(A, kg/(mol s)	$\Delta S^‡$ cal/(Kmol) (T = 200 °C)	ν(CN) cm^{-1}
CH_3−	30.4 ± 0.7	27.7 ± 0.7	−6.4	2254
	26.5[a]	23.8	−14	
CH_3CH_2−	21.5 ± 0.3	19.7 ± 0.4	−22	2247
	25.6[b]	23.2	−15	
$(CH_3)_2CH$−	19.7 ± 0.9	17.8 ± 1	−26	2241
$HOC(O)CH_2$−	34.7 ± 0.5	33.7 ± 0.5	5.4	2265
	26.3[a]	22.8	−16	

[a] Calculated from ref 11. [b] Calculated from ref 10.

The time derivative of $[H^+]$ (eq 12) based on the charge balance provides $[H^+]$ throughout the reaction. The rate constants at each temperature were determined by assuming the steady-state condition for the amide concentration.

$$\frac{d[H^+]}{dt} = \left\{\frac{d[B_T]}{dt}\left[\frac{K_a}{K_a + [H^+]} - \frac{[H^+]}{K_b + [H^+]}\right]\right\} \Bigg/ \left(1 + \frac{B_T}{K_b + [H^+]} - \frac{B_T^2[H^+]}{(K_b + [H^+])^2} + \frac{K_W}{[H^+]^2} + \frac{K_aB_T}{(K_a + [H^+])^2} + \frac{K_cC_T}{(K_c + [H^+])^2}\right) \quad (12)$$

Figure 6 shows the fitted values for the disappearance of $(CH_3)_2CHCN$ (k_1') and the calculated values for the appearance of the carboxylic acid and ammonia products at 240 °C. The model demonstrates that as $[H^+]$ decreases, reaction 3 slows down and eventually stops. Table 2 gives the rate constants for each nitrile at the temperatures studied. The Arrhenius parameters are listed in Table 3 and will be discussed further below.

The kinetics of acid-catalyzed hydrothermolysis of cyanoacetic acid were solved in the same way as for the alkyl nitriles with a few exceptions. The concentration of acetamide in Scheme 2 was assumed to be small and in steady state. Because the rate of decarboxylation of malonamic acid was found to be the same with and without added HCl, the uncatalyzed rate determined previously[31] was used.

The charge balance for Scheme 2 is given by eq 13.

$$[Cl^-] + [H_2NC(O)CH_2CO_2^-(MMA)] + [NCCH_2CO_2^-(CAA)] + [CH_3CO_2^-] + [OH^-] + [HCO_3^-] = [H^+] + [NH_4^+] \quad (13)$$

In arriving at eq 13, it was determined that the contribution of

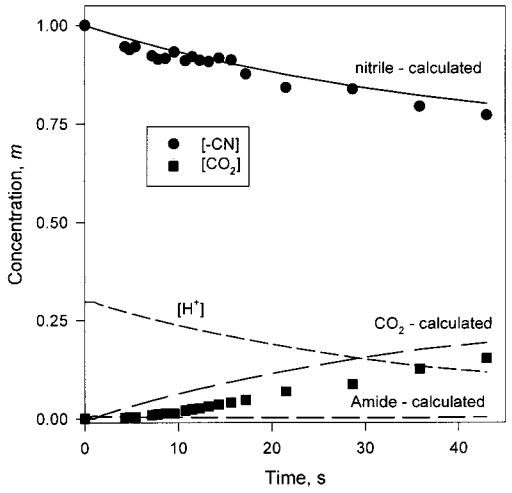

Figure 7. Calculated and observed concentrations for 1.0 *m* $NCCH_2CO_2H$ in 0.3 N HCl at 190 °C under 275 bar.

MMA and CAA anions had to be included even though their concentrations were small. CO_2 is produced, which necessitates the inclusion of HCO_3^- in the charge balance, even though the solution is acidic and the HCO_3^- contribution is very small. When the charge balance equation is redefined in terms of $[H^+]$, the time derivative of $[H^+]$ is given by eq 14 and is slightly more complicated than eq 12.

$$\frac{d[H^+]}{dt} = \left\{ \frac{d[CAA]}{dt}\left(\frac{K_{CAA}}{[H^+]}\right) + \frac{d[MMA]}{dt}\left(\frac{K_{MMA}}{[H^+]}\right) + \frac{d[CO_2]}{dt}\left(\frac{K_{CO_2}}{[H^+]}\right) + \frac{d[B_T]}{dt}\left[\frac{K_a}{K_a + [H^+]} - \frac{[H^+]}{K_B + [H^+]}\right]\right\} \Bigg/ \left(1 + \frac{B_T}{K_b + [H^+]} - \frac{B_T^2[H^+]}{(K_b + [H^+])^2} + \frac{K_W}{[H^+]^2} + \frac{K_a B_T}{(K_a + [H^+])^2} + \frac{[CAA]K_{CAA}}{[H^+]^2} + \frac{[MMA]K_{MMA}}{[H^+]^2} + \frac{K_c C_T}{(K_c + [H^+])^2}\right) \quad (14)$$

As before $B_T = A_T$. With $d[H^+]/dt$ now available, the nitrile hydrolysis rate constants can be determined at each temperature. Since the reactant nitrile band and CO_2 were both visible in the IR flow cell, each temperature was solved minimizing the error (χ^2) on both compounds (Figure 7). The focus was on fitting the concentration data for the nitrile with the most accuracy because the rate for the nitrile hydrothermolysis, k_1' (step B in Scheme 2), is the most important unknown for this work. Because of the rather low absorptivity of the −CN stretch (Figure 4), fitting uncertainties lead to some error in the CO_2 concentration. Arrhenius parameters are given in Table 3 along with those calculated from previous rate measurements in the normal liquid range of H_2O.[10,11] These parameters differ significantly from the lower temperature regime, but because of the kinetic compensation effect between E_a and A, the rates are comparable (Figure 8).

Structure−Reactivity Relations. A rough correlation exists in Table 3 between the increasing −CN stretching frequency and the activation energy as a function of R. This observation suggests that the Taft eq 15 might provide additional insight into the role of the steric, E_s, and electronic, σ^*, properties of R in the nitrile hydrothermolysis rate.[38] In eq 15,

$$\log(k/k_0) = \delta E_s + \rho\sigma^* \quad (15)$$

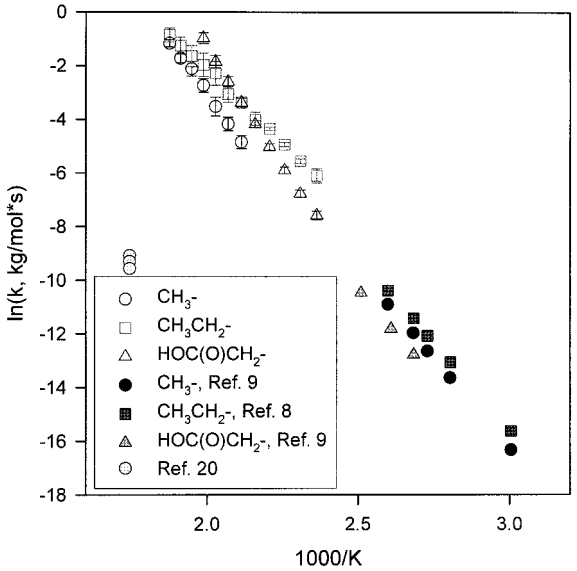

Figure 8. Arrhenius plot of the alkyl nitriles and cyanoacetic acid compared to the literature values for the same compounds.

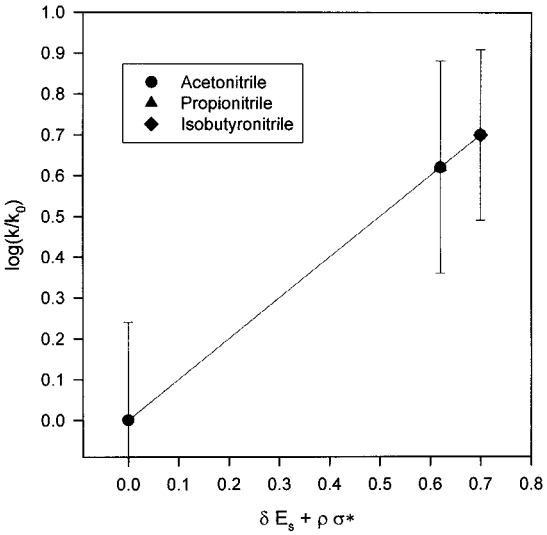

Figure 9. Taft plot for the rate of hydrothermolysis of the alkyl nitriles compared to CH_3CN at 200 °C in which $\rho = -7.2$ and $\delta = 1.4$.

k_0 is the rate constant of the reference compound, which in this case was chosen to be acetonitrile. The substituent constants used for the R groups are given in Table 1. δ and ρ are the weighting coefficients that were adjusted to optimize the fit between the substituent constants and the rate constants. Figure 9 shows the plot that results for the simple alkyl nitriles. The values of $\rho = -7.2$ and $\delta = 1.4$ thus obtained suggest that increasing the electron-donating character of R causes the rate to increase to a greater extent than increasing its steric bulk. This observation is consistent with the qualitative correlation between E_a and ν(CN) in Table 3, which implies that the electronic inductive effect of R dominates in determining the reaction rate. Figure 9 does not include $NCCH_2CO_2H$ because its hydrolysis rate is much faster at hydrothermal conditions than would be predicted from the correlation in Figure 9 for simple alkyl nitriles. A possible explanation is that the protonated nitrile group and H_2O can form a six-membered ring with the carboxylate group in $NCCH_2CO_2H$, which facilitates nucleophilic attack by water on the electropositive nitrile carbon atom. The absence of the carboxylate group in the simple alkyl

nitriles precludes this type of stable transition state, which results in a slower rate of hydrolysis.

Conclusions

The mechanism of hydrothermolysis of simple alkyl nitriles in the presence of HCl is easily modeled with two forward reactions and one equilibrium step. When two reactive functional groups are present in the molecule, the method of real-time spectroscopy makes it possible to define and follow competitive, pH-sensitive reactions.

The rates of hydrothermolysis of simple alkyl nitriles in water at the temperature and pressure conditions of a submarine hydrothermal vent are probably too slow to be of importance in the absence of a catalyst. Hydrogen ions accelerate the reaction. Hence the kinetics, as well as previously discussed concentration considerations,[5] argue against the Strecker reaction as having a major role in the hydrothermal vent. Likewise, the destruction of nitriles in waste streams will benefit from the intentional addition of a strong acid.

Acknowledgment. We are grateful to the Army Research Office (Robert W. Shaw, Program Manager) for financial support of this work on DAAG55-98-1-0253 and to Dr. Bill Izzo for helpful discussions about nitrile kinetics.

References and Notes

(1) Miller, S. L. *Biochim. Biophys. Acta* **1957**, *23*, 480.
(2) Miller, S. L.; Van Trump, J. E. In *Origins of Life*; Wolman, Y., Ed.; D. Reidel Publishing Co.: Dordrecht, The Netherlands, 1981; p 135.
(3) Peltzer, E. T.; Bada, J. L.; Schlesinger, G.; Miller, S. L. *Adv. Space. Res.* **1984**, *4*, 69.
(4) Cronin, J. R.; Chang, S. In *The Chemistry of Life's Origin*; Greenberg, J. M., Pirronella, V., Eds.; Kluwer Academic: Dordrecht, The Netherlands, 1993; p 209.
(5) Schulte, M.; Shock, E. *Origins Life Evol. Biosphere* **1995**, *25*, 161.
(6) Haymon, R. M.; Macdonald, G. N. *Am. Sci*. **1985**, *73*, 441.
(7) Rona, P. A., Bostrom, K., Laubier, L., Smith, K. L., Eds. *Hydrothermal Processes at Sea Floor Spreading Centers*; Plenum: New York, 1984.
(8) De Leer, E. W. B.; Simninghe Damste, J. S.; Erkelens, C.; De Galan, L. *Environ. Sci. Technol*. **1985**, *19*, 512.
(9) Krieble, V. K.; Noll, C. I. *J. Am. Chem. Soc.* **1939**, *61*, 560.
(10) Rabinovitch, B. S.; Winkler, C. A. *Can. J. Res.* **1942**, *20A*, 221.
(11) Rabinovitch, B. S.; Winkler, C. A.; Stewart, A. R. P. *Can. J. Res.* **1942**, *20B*, 121.
(12) Sullivan, M. J.; Kilpatrick, M. L. *J. Am. Chem. Soc.* **1945**, *67*, 1815.
(13) Kilpatrick, M. L. *J. Am. Chem. Soc.* **1947**, *69*, 40.
(14) Liler, M.; Kosanovic, D. *J. Chem. Soc.* **1958**, 1084.
(15) Mujumdar, G. G.; Dole, K. K.; Karve, D. D. *J. Univ. Bombay, Sci.* **1947**, *16A* (3), 25.
(16) Tsai, L.; Miwa, T.; Newman, M. S. *J. Am. Chem. Soc*. **1957**, *79*, 2530.
(17) Taylor, T. W. J. *J. Chem. Soc*. **1930**, 2741.
(18) Harrell, C. L.; Klein, M. T.; Adschiri, T. *Adv. Environ. Res*. **1998**, *1*, 373.
(19) Izzo, B.; Harrell, C. L.; Klein, M. T. *AIChE J*. **1997**, *43*, 2048.
(20) Harrell, C. L. Investigation and Modeling of Nitrile Hydrothermal Chemistry: Physical and Chemical Effects. Ph.D. Dissertation, University of Delaware, Newark, DE, 1998.
(21) Katritzky, A. R.; Lapucha, A. R.; Siskin, M. *Energy Fuels* **1990**, *4*, 560.
(22) Schoppelrei, J. W.; Kieke, M. L.; Wang, X.; Klein, M. T.; Brill, T. B. *J. Phys. Chem*. **1996**, *100*, 14343.
(23) Kieke, M. L.; Schoppelrei, J. W.; Brill, T. B. *J. Phys. Chem.* **1996**, *100*, 7455.
(24) Schoppelrei, J. W.; Kieke, M. L.; Brill, T. B. *J. Phys. Chem.* **1996**, *100*, 7463.
(25) Schoppelrei, J. W.; Brill, T. B. *J. Phys. Chem. A* **1997**, *101*, 2298.
(26) Schoppelrei, J. W.; Brill, T. B. *J. Phys. Chem. A* **1997**, *101*, 8598.
(27) Maiella, P. G.; Brill, T. B. *Inorg. Chem.* **1998**, *37*, 454.
(28) Maiella, P. G.; Brill, T. B. *J. Phys. Chem.* **1996**, *100*, 14352.
(29) Maiella, P. G.; Brill, T. B. *J. Phys. Chem. A* **1998**, *102*, 5886.
(30) Belsky, A. J.; Brill, T. B. *J. Phys. Chem. A* **1998**, *102*, 4509.
(31) Belsky, A. J.; Maiella, P. G.; Brill, T. B. *J. Phys. Chem. A*, submitted.
(32) Galat, A. *J. Am. Chem. Soc*. **1948**, *70*, 2596.
(33) Maiella, P. G.; Schoppelrei, J. W.; Brill, T. B. *Appl. Spectrosc*., in press.
(34) Cutler, A. H.; Antal, M. J., Jr.; Jones, M., Jr. *Ind. Eng. Chem. Res*. **1988**, *27*, 691.
(35) Cvetanovic, R. J.; Singleton, D. L. *Int. J. Chem. Kinet.* **1977**, *9*, 481.
(36) Cvetanovic, R. J.; Singleton, D. L. *Int. J. Chem. Kinet.* **1977**, *9*, 1007.
(37) Belsky, A. J.; Li, T.; Brill, T. B. *J. Supercrit. Fluids* **1997**, *10*, 201.
(38) Taft, R. W., Jr. *Steric Effects in Organic Chemistry*; Newman, M. S., Ed.; John Wiley and Sons: New York, 1956.
(39) Perrin, D. D.; Dempsey, B.; Serjeant, E. P. *pK_a Prediction for Organic Acids and Bases*; Chapman and Hall: London, 1981.
(40) Unger, S. H.; Hansch, C. *Prog. Phys. Org. Chem*. **1976**, *12*, 91.
(41) Gal, E. M.; Shulgin, A. T. *J. Am. Chem. Soc*. **1951**, *73*, 2938.
(42) Liler, M. *Reaction Mechanisms in Sulfuric Acid and Other Strong Acid Solutions*; Academic Press: London, 1971; Vol. 23.
(43) Foy, B. R.; Waldthausen, K.; Sedillo, M. A.; Buelow, S. J. *Environ. Sci. Technol*. **1996**, *30*, 2790.
(44) Darensbourg, D. J.; Holtcamp, M. W.; Longridge, E. M.; Khandelwal, B.; Klausmeyer, K. K.; Reibenspies, J. H. *J. Am. Chem. Soc*. **1995**, *117*, 318.
(45) Hall, G. A., Jr. *J. Am. Chem. Soc*. **1950**, *72*, 4709.
(46) Meyer, J. C.; Marrone, P. A.; Tester, J. W. *AIChE J*. **1995**, *41*, 2108.
(47) Boock, L. T.; Klein, M. T. *Ind. Eng. Chem. Res*. **1993**, *32*, 2464.
(48) Schaeffer, F. C. In *The Chemistry of the Cyano Group*; Rappoport, Zvi, Ed.; John Wiley and Sons: New York, 1970.
(49) Olah, G. A.; Kiovsky, T. E. *J. Am. Chem. Soc*. **1968**, *90*, 4666.
(50) Kortum, G.; Vogel, W.; Andrussow, K. *Dissociation Constants of Organic Acids in Aqueous Solution*; Butterworths: London, 1961.
(51) Subcommittee on Ammonia. *Ammonia*; University Press: Baltimore, MD, 1979.
(52) Lindsay, W. T., Jr. *Proc. Int. Conf. Eng. W. Pa*. **1980**, *41*, 284.
(53) Marshall, W. L.; Franck, E. U. *J. Phys. Chem. Ref. Data* **1981**, *10*, 295.